Kiselev, Hahn, Auer:

Is the Brain Cortex a Fractal?

Sonderforschungsbereich 386, Paper 297 (2002)

Online unter: http://epub.ub.uni-muenchen.de/

Is the Brain Cortex a Fractal?

Valerij G. Kiselev[*], **Klaus R. Hahn**[†], **and Dorothea P. Auer**[‡],

[*] Institute of Medicine, Research Center Jülich,
present address: Section of Medical Physics, Department of Diagnostic Radiology, University Hospital Freiburg, Freiburg, Germany.
Corresponding author, e-mail: kiselev@ukl.uni-freiburg.de .
[†] Max Plank Institute of Psychiatry, Munich, Germany.
[‡] Institute of Biomathematics and Biometry, GSF, Research Center for Environment and Health, Oberschleissheim, Germany.

Running title: Is the Brain Cortex a Fractal?

Address for Correspondence:

Dr. Valerij G. Kiselev
Section of Medical Physics
Department of Diagnostic Radiology
University Hospital Freiburg
Hugstetterstr. 55
D-79102 Freiburg, Germany

Tel.: +49 761 2705182
Fax: +49 761 2703831
E-mail: kiselev@ukl.uni-freiburg.de

Abstract

The question is analysed if the human cerebral cortex is self-similar in a statistical sense, a property which is usually referred to as being a fractal. The presented analysis includes all spatial scales from the brain size to the ultimate image resolution. Results obtained in two healthy volunteers show that the self-similarity does take place down to the spatial scale of 2.5 mm. The obtained fractal dimensions read $D = 2.73 \pm 0.05$ and $D = 2.67 \pm 0.05$ correspondingly, which is in a good agreement with previously reported results. The new calculational method is volumetric and is based on the fast Fourier transform of segmented three-dimensional high-resolved magnetic resonance images. Engagement of FFT enables a simple interpretation of the results and achieves a high performance, which is necessary to analyse the entire cortex.

1 Introduction

The complexity of the cerebral cortex geometry suggests a description based on the notion of fractal, a mathematical construction dedicated to describe the self-similarity of various objects in dead and living nature (see, e.g., Liu, 1986, a brief introduction into the notion of fractal is given below). The first question to be answered on this way is whether the cortex is indeed self-similar. This would mean that the statistical properties of the gyrification pattern of small cortex structures are similar to that of the large ones. This approach refers to averaged characteristics of the brain in contrast to the precise anatomic description of individual structures.

The present problem has its own history. Hofman (Hofman, 1991) gave a strong argument in favour of the fractal geometry of the human cortex based on a surface-to-volume relation in the mammalian brains. Majumdar and Prasad (Majumdar and Prasad, 1988) found a fractal dimension $D = 2.60 \pm 0.5$ for the external cortex surface in the normal subjects. The performed analysis was based on magnetic resonance (MR) images of brain sections with a unity added to the final result. A three-dimensional analysis of a fixed brain specimen was performed by Chuang et al. (Chuang et al., 1991) with the result $D = 2.20$. Both studies were criticized by Free et al. (Free et al., 1996). They investigated the interface between the human white and grey matter obtained from segmented volumetric MR data. They found that a smoothing of the white matter surface reduces its area in agreement with the hypothesis of the fractal geometry and found a corresponding fractal dimension $D = 2.30 \pm 0.01$. Note that this fractal dimension was obtained from five smoothing levels the extent of which ranged from 1.4 to 6.1 mm with the original voxel size interpolated to $0.47 \times 0.47 \times 0.36$ mm^3. This result does support the hypothesis that the white matter surface has a fractal geometry, but the small amount of smoothing levels does not allow to conclude about its entire geometry.

Although plausible the property of being a fractal needs to be verified. In this paper we analyse the geometry of the human cortical grey matter. We find a range of spatial scales in which the grey matter arrangement is self-similar and calculate the fractal dimensions in this range. This is enabled by a new computational method, which is suitable for fast automated analysis of given cortices over the whole range of spatial scales.

2 Materials and Methods

2.1 A Brief Introduction to Fractal Geometry

Let us briefly review the properties of fractals which are essential for the present study. The notion of dimensionality stems from the everyday experi-

ence. For example, a thin wire is one- and a sheet of paper is two-dimensional. A mathematical definition, that digests this common sense, can be formulated as follows. Consider an object, the dimension of which is to be determined. One has to take an element of this object. The element may be for example a voxel or a molecule. One has to surround it with a sphere of a given radius R and count the amount of object elements v inside the sphere. The measure of v can be arbitrary, it can be, for example, the amount of voxels or the volume. Of importance is only the dependence of v on the sphere radius upon averaging over the elements put in its origin. This value scales as $v \propto R^D$ where D is the dimension by definition. This definition not only resolves the expected dimensions in the simplest cases mentioned above, but also takes into account the fact that the relevant dimension of an object depends on the spatial scale. For example both the wire and the paper sheet show the dimension of three at short distances for which the sphere radius R is smaller than their thickness. At higher R a transition to the dimensions of one or two occurs. Thus even the simplest examples instructively highlight the importance of crossovers in the dependence of the dimension on the spatial scale R. These change points indicate the characteristic lengths which are present in the investigated object.

The above definition can be reformulated in order to become a practical mathematical tool. The average amount of matter v in the sphere of radius R is equal to

$$v(R) = \int \rho(\mathbf{r}) d^3 r, \tag{1}$$

where $\rho(\mathbf{r})$ is the probability to find two object elements at the separation $\mathbf{r}$ and the integration is performed over the sphere volume. The function $\rho(\mathbf{r})$ provides a detailed description of the geometry of the considered object. This function is known under different names in many physical contexts. Here we refer to it as the density-density correlation function, the name borrowed from the condensed matter physics.

Consider objects, which are isotropic in the statistical sense. The above definition of the fractal dimension with account for eq. (1) requires ρ to depend on a power of r, the absolute value of the vector $\mathbf{r}$: $r = |\mathbf{r}|$.

$$\rho(\mathbf{r}) = \mathrm{Const} \cdot r^{D-3}. \tag{2}$$

Self-similarity is the second issue involved in the present analysis. It implies that the object looks similar to its zoomed part. The words "looks similar" demand a proper mathematical definition. As such, one requires that at least the density-density correlation functions derived from the main and the zoomed images have the same form. In view of eq. (2) this means an invariance of the object dimension D with respect to zooming.

The fractals are nontrivial self-similar objects. The trivial ones are, for ex-

ample, a straight line, a plane or three-dimensional space. The dimension D for fractals takes fractional values hence the name. For any example, which exists in Nature, one can find a range of spatial scales over which the fractal geometry holds. For example the coast line remains a fractal over the lengths from the island size to that of a single rock. In the present study a special attention is paid to inspecting the self-similarity range of the human cerebral cortex.

2.2 Analysis of Cortex Geometry

The presented method refers to the density-density correlation function $\rho(\mathbf{r})$, which, for the case of the cerebral cortex is the probability to find two voxels in the cortex separated by a given vector $\mathbf{r}$. In fractals this function scales according to eq. (2) as r^{D-3}, where $r = |\mathbf{r}|$ and D is the fractal dimension. This dependence yields a straight line when plotted in the double logarithmic scale. The reported method is applied to segmented brain images (obtained as described below), in which the grey matter is assigned a value of unity, while the brightness of all other voxels is set to zero.

In principle, calculation of $\rho(\mathbf{r})$ is possible via a straightforward voxel counting in the segmented brain images. However this procedure results in a huge number of operations of the order of N^2 where N is the total number of voxels. For a high-resolution anatomical MR images as those used in the present study $N \approx 2^{26}$ and the data processing becomes extremely time-consuming. The same problem is inherent in the previous approaches based on measuring the cortical area (Majumdar and Prasad, 1988; Chuang et al., 1991; Free et al., 1996).

We solve this problem by working with the Fourier transform $f(\mathbf{k})$ of the segmented cortex from which we recollect the necessary information about the correlation function $\rho(\mathbf{r})$. The use of the fast Fourier transform (FFT) helps to avoid a huge amount of computations, since it requires only about $N \ln N$ operations. The gain in performance for the high-resolution anatomical images is two orders of magnitude.

For the analysis the squared magnitude $|f(\mathbf{k})|^2$ is averaged over the directions of the wave vector $\mathbf{k}$. This yields a function $F(k)$ which is real and depends only on the absolute value $k = |\mathbf{k}|$:

$$F(k) = \frac{1}{4\pi} \int |f(\mathbf{k})|^2 d\Omega_k, \tag{3}$$

where $d\Omega_k$ integrates over two angles, that define the direction of vector $\mathbf{k}$.

As shown in the Appendix, $F \propto k^{-D}$ for fractals. Thus a straight segment in the double logarithmic plot of $F(k)$ indicates a self-similarity range of the cortex. There might be several straight sections with different values of D.

The cross-overs between them indicate scales at which the cortex geometry changes.

2.3 MR Brain Imaging

Magnetic resonance images were obtained at 1.5 T scanner (GE Medical Systems). High resolution, whole brain T1-weighted spoiled gradient echo-datasets (SPGR, IR-PREPPED, repetition time (TR) = 10.3 ms, echo time (TE) = 3.4 ms, field of view (FOV) = 23×23 cm^2, matrix size = 256×256, flip angle = 20^o) were acquired in the sagittal plane with an in-plane resolution 0.90×0.90 mm^2. Three-dimensional data sets consisted of 128 contiguous slices of thickness 1.3–1.4 mm. Two young healthy normal volunteers were included in this study.

2.4 Image Segmentation

The grey matter was segmented from the measured data by a method which was published in preliminary versions in several proceedings (Hahn et al., 2000, 2001a,b), a more detailed description of an essentially improved variant including validation examples is submitted for publication. This nonparametric intensity segmentation method eliminates after skull pealing via several correction steps distortion and noise artifacts. Finally, after nonlinear edge preserving noise elimination global thresholds are introduced to separate CSF, grey and white matter. In case of data with a large grid cell width d, the boundary surface between white and grey matter is smoothed to avoid irregular blocking effects on small scales, before introducing global thresholds. To achieve that, the corrected data are interpolated to a finer grid (e.g. $d/2$) and then smoothed by a narrow Gaussian filter (standard deviation= $d/2$). No shape prior is used, so the method applies equally well to normal and malformed brains. The main new features are axial and irregular bias corrections which are based on an estimate of the cortex distortions in contrast to the frequently used white matter based corrections with subsequent extrapolation to the cortex, see e.g. (Dale et al., 1999). The nonequivalence of grey or white matter based distortion fields is one of the interesting outcomes of this segmentation study (Hahn et al., 2001a,b). This method is especially well suited for the present fractal analysis, as the considered measure is derived from volumetric cortex properties and as the cortex distortions are removed with higher precision than those in white matter. The method requires few user interactions to control the parameter settings, by renunciation of a perfect automaticity it gains flexibility and precision. To test precision, the Montreal brain phantom (Kwan et al., 1996; Cocosco et al., 1997) was segmented for a noise level of 3% and a distortion of 40% RF nonuniformity, which roughly approximates the distortions in our real data. A quantitative measure of the

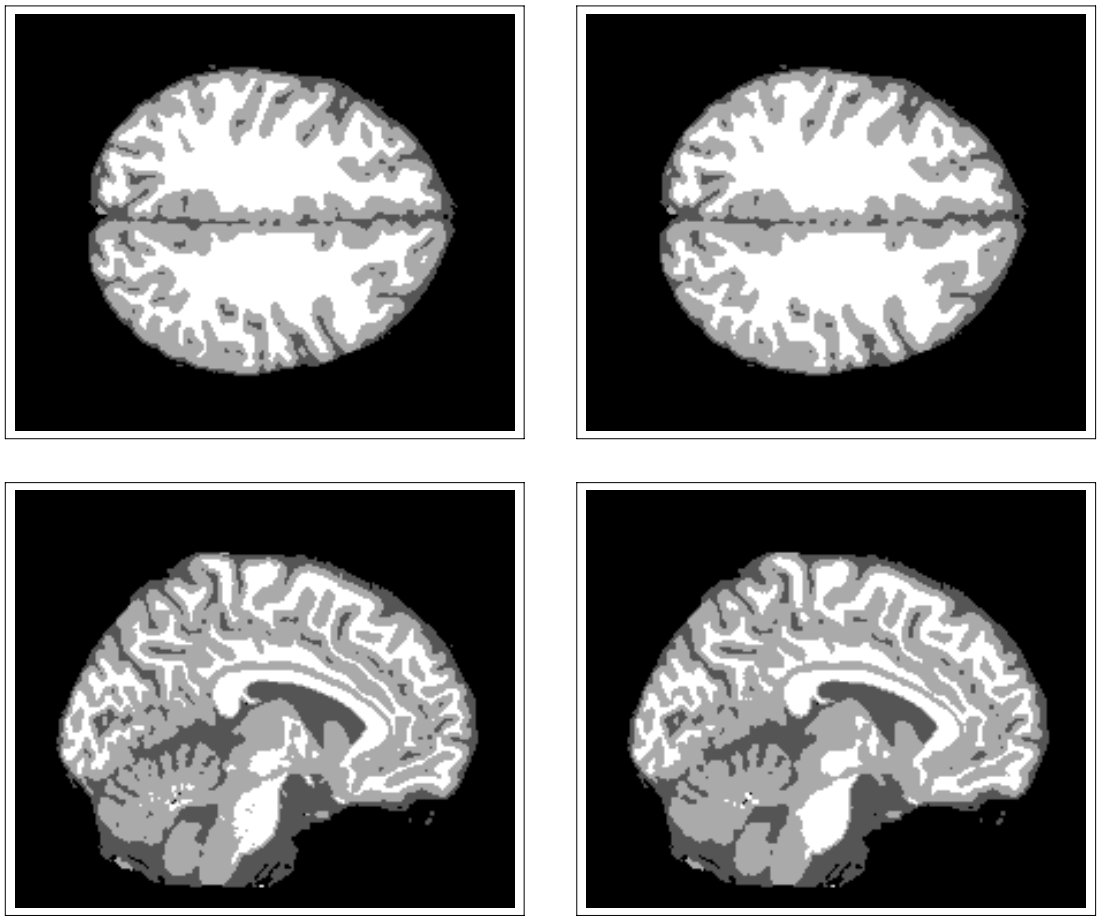

Fig. 1.
CSF, grey and white matter of an axial and a sagittal slice in obvious coloring. Left panels show the labeling of the Montreal brain phantom, right panels the thresholded result of the segmentation method applied to the phantom with a 3% noise level and with 40% RF nonuniformity.

segmentation quality is given by a κ-statistics (Ashburner and Friston, 2000), measuring the separation of CSF, grey and white matter for the whole brain. The presented segmentation method improves $\kappa = 0.913$ for the distorted and noisy phantom to $\kappa = 0.962$. A recently published value of $\kappa = 0.95$ achieved by the SPM method (Ashburner and Friston, 2000) indicates this to be a good quality. This is also exemplified by Figure 1 where the segmentation result for an axial and a sagittal slice is compared to the corresponding phantom tissues.

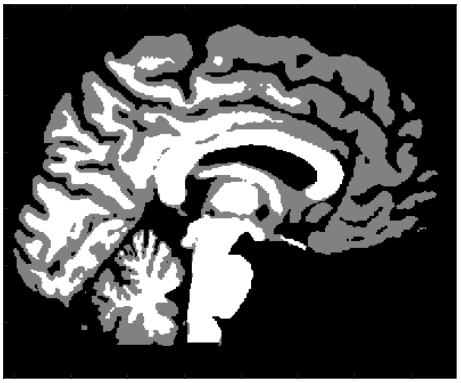

Fig. 2.
Segmented sagittal slice in Volunteer 1. White matter and the cerebellum were removed before further processing.

2.5 Analysis of Geometry

The segmented images had a doubled resolution ($d/2$) of $512 \times 512 \times 256$ voxels with the voxel size $0.45 \times 0.45 \times 0.5\text{mm}^3$. The white matter and the cerebellum were removed. The resulting grey matter (GM) maps contained only the cortical and subcortical GM voxels with unitary brightness. These images were Fourier transformed with an FFT routine resulting in function $f(k)$, eq. (3). The integration in eq. (3) was performed numerically by subdividing k-space in a number of spherical shells with logarithmically spaced thickness and computing the average k and $F(k)$ in each shell. The fractal dimension was found by fitting a linear function to the dependence of $\lg F$ on k. All computations were performed with house-written C programs.

3 Results

An example of a segmented sagittal slice is shown in Figure 2. There are minor artifacts, such as the grey matter layer at the brain stem or a small GM island near the cerebellum. The GM maps also contained the striatum and parts of other subcortical nuclei. Their effect on the final result is negligible however due to their low statistical weight as compared to the correctly segmented cortical GM voxels.

Plots of the function $F(k)$ are shown in Figure 3. The presence of an initial straight segment suggests that the cortex geometry is self-similar up to $k = 1.3$ mm^{-1}. The corresponding length defined as π/k is 2.5 mm. The fractal dimensions in this range were found by fitting a linear function to the data points from the 1st to the 36th (which corresponds to the above given value of k). The results for two volunteers were $D = 2.73 \pm 0.05$ and $D = 2.67 \pm$

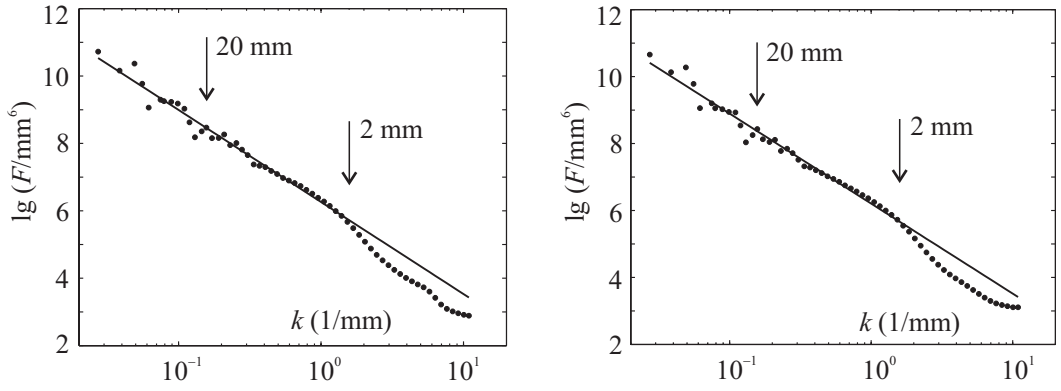

Fig. 3.
The function $\lg F(k)$ plotted v.s. k which is shown in the logarithmic scale for both volunteers. The straight lines show the result of an equal-weight fitting of the formula $\lg F(k) = Const - D \lg k$ to the data for the points through 1st to 36th. This gives the fractal dimension $D = 2.73 \pm 0.04$ (left) and $D = 2.67 \pm 0.04$ (right). The arrows indicate the values of k which correspond to given structure sizes in real space defined as π/k. The errors in the data are discussed in the text.

0.05 (error bar at one standard deviation of the fitting result, correlation coefficients of the linear fit R = 0.9998 in both cases). The actual accuracy of the calculated fractal dimension is smaller due to the ambiguity in the interval in which the fitting is performed. For example, an application of the fitting only to the data points from the 18th to the 36th (Figure 3) results in $D = 2.59 \pm 0.04$ (R = 0.99996) and $D = 2.41 \pm 0.03$ (R = 0.99998). The corresponding intervals in Fourier and real spaces are 0.23–1.27 mm^{-1} and 13.6–2.5 mm respectively.

4 Discussion

The main result of the performed study is that the human cerebral cortex does show a nearly fractal geometry down to the spatial scale of 2.5 mm. This limit reasonably corresponds to the cortex thickness. At larger k a finer spatial scale is probed at which the cortex is not subjected to folding.

The coarse spatial scale (small k in Figures 3) is described with poor statistics. This follows from small numbers of grid points in Fourier space, which are averaged by computing individual F-values (Figure 4). One could expect that the shape of the $F(k)$ curve in this range is determined by the overall cortex structure, which is not subjected to statistical averaging involved in the definition of the fractal dimension. In contrast to these expectations, the self similarity of the cortex folding sets up already for the largest spatial scales as

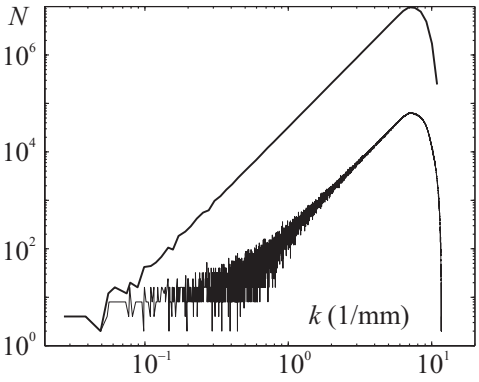

Fig. 4.
Number of data points involved in the averaging over the orientations of the wave number k in computing $F(k)$. The upper line is obtained for 59 intervals presented in Figures 3, left. The lower line shows the same value for 5870 intervals. F(k) for this case is presented in Figure 7 The coinciding initial parts of both lines are determined by a few grid points near the origin of k-space. The slope of their main parts shows the dependence $N \propto k^3$. To explain this exponent, note that each k-interval represent a thin spherical shell of radius k selected in three-dimensional k-space. The shell surface increases quadratically, and its thickness is proportional to k for the used logarithmic spacing. The drop at large k is due to the rectangular shape of sampled k-space.

suggested by the averaged linear behaviour seen in Figure 3 for the smallest k.

4.1 Comparison with Spherical Geometry

Let us compare the function $F(k)$ characterizing the cortical geometry with that for a sphere of radius R. The latter takes the form

$$F(k) = \left(\frac{4\pi R}{k^2}\right)^2 \left(\cos kR - \frac{\sin kR}{kR}\right)^2 \tag{4}$$

We selected $R = 67$ mm in order to match the peculiarities seen for low k data points in Figure 3. This value reasonably matches the brain size. Both dependencies are shown in Figure 5. Although similar for the initial few points, the curves significantly differ from each other. First, the overall slope set by the first factor in eq. (4) is equal to -4. Second, the oscillating factor in eq. (4) results in many dips, which are asymmetric in logarithmic scale. The apparent irregular shape of the sphere $F(k)$ is due to an insufficient sampling of an oscillating line. The number of periods of the second factor in eq. (4) is close to 11 for $k = 1$ mm^{-1}. This comparison suggests that the peculiarities seen in the left Figure 3 at small k do not originate from any noise. Rather

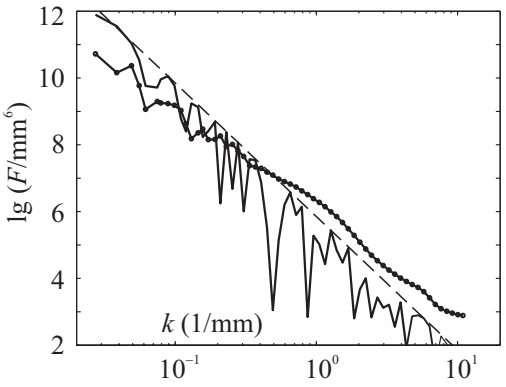

Fig. 5.
A comparison of $F(k)$ for the cortex (the same line as shown in the left Figure 3 with $F(k)$ calculated for a sphere of radius 67 mm eq. (4) (the irregular line). The dashed line shows the first non-oscillating factor in eq. (4).

they can be attributed to the overall brain shape. The same conclusion is suggested by the similarity of $F(k)$ for two subjects seen in Figure 3.

Equation (3) shows that the residual deep grey matter, which is included in the processed images, does not significantly affect the results. First, it has a lower volume, which defines its contribution to $F(0)$ (point $k = 0$ is not shown in Figures 3 – 7). Second, it is unfolded, which suggests a decrease in its contribution to scale as k^{-4}. Thus its relative contribution to the fractal dimension can be estimated as a square ratio of its volume to the cortical one. The volume of basal ganglia are known to be less than 2.5% of the intracranial volume Gunning-Dixon et al. (1998) and the total GM including basal ganglia and cerebellum in young adults was estimated as 53.7% Kaufmann et al. (2002). The above estimate takes the form $(2.5/53.7)^2 = 2.2 \times 10^{-3}$. Such a contribution in the fractal dimension can be neglected as it is smaller than the fit error.

4.2 More Details about Data Averaging

The coarse brain structure clarifies the origin of the apparently large error in the data presented in Figures 3. Figure 6 shows the error corridor for the data presented in the left Figure 3. The error bars were obtained as the standard deviation σ of the F-values upon averaging in each k-interval. The nearly constant $\sigma(k)$ rules out a purely random origin. Indeed, the number of averaged voxels enormously increases for large k as shown in Figure 4. The conventional averaging of randomized deviations would result in a fast decreasing $\sigma(k)$. Why this is not the case can be explained by the following reasons. Consider an idealized cortex having an overall shape of an ellipsoid and the folding of which is similar in any direction from its center. Consider the function $|f(\mathbf{k})|^2$

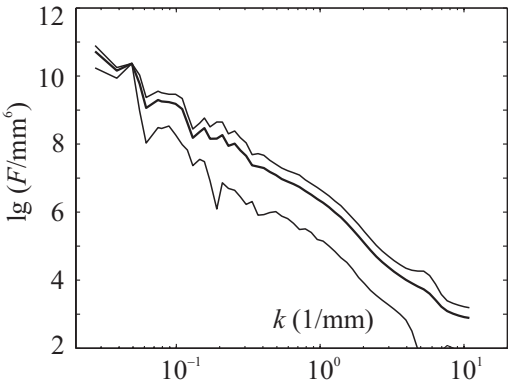

Fig. 6.
Apparent errors in data shown in the left Figure 3. The middle line reproduces the function $\lg F(k)$. The error corridor is formed by the standard deviation σ of data averaged to obtain the values attributed to each k-interval. Its magnitude is typically close to that of $F(k)$ and it marginally depends on k. The upper line shows $\lg[F(k) + \sigma(k)]$. The lower line presents $\lg F(k) - \sigma(k)/F(k)$. The latter formula coincides with $\lg[F(k) - \sigma(k)]$ for small $\sigma(k)$ and helps avoiding negative values in the logarithmic scale. A deterministic origin of this seemingly large error is discussed on the text.

eq. (3), which results in $F(k)$ after averaging over the direction of vector $\mathbf{k}$. The dependence $|f(\mathbf{k})|^2$ plotted against k would show a fractal dimension, which would be the same for all directions of vector $\mathbf{k}$. At the same time, the magnitude of $|f(\mathbf{k})|^2$ would be different in different directions according to the ellipsoid shape. The $F(k)$ values are obtained by the angular averaging in eq. (3). In the considered example, this would be an averaging of many parallel lines with a significant spreading in their offsets. It would result in a constant $\sigma(k)$ similar to one presented in Figure 6. For the ellipsoid, this effect could be corrected by an appropriate rescaling of, e.g., k_x and k_y. For real cortex, this is difficult due to its more complicated structure even at the coarser spatial scales.

The above reasoning is supported by data presented in Figure 7 showing the effect of a finer k-gridding by computing the function $F(k)$. Treating of $F(k)$ with less k-intervals leads to more averaged values in each of them, while the smaller intervals present more individual contributions. Practically an apparently smooth $F(k)$ emerges when the number of averaged data point reaches one hundred, as it is seen from comparison of Figures 7 and 4. The averaging, which is not performed in the fine k-intervals, is effectively done later by fitting performed for computing the fractal dimension. One can initially calculate more averaged $F(k)$ or let this job be done by fitting. These ways are not equivalent though. The former methods works with $F(k)$, thus complying with the definition of fractal dimension, while in the latter the effectively averaged quantity is $\lg F(k)$. The averaging of logarithm should yield a smaller

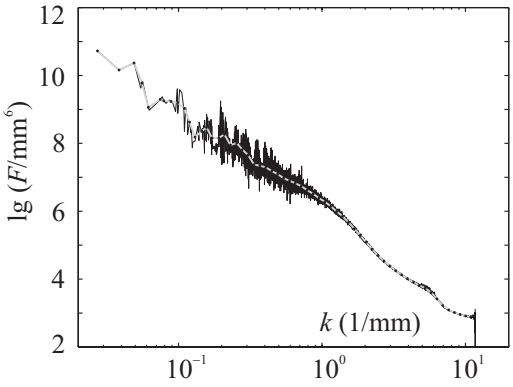

Fig. 7.
Effect of reducing the k-intervals in computing $F(k)$. The grey line with black points presents the same data as in the left Figure 3. The less regular black line shows $F(k)$ for a subdivision of k-axis in 5870 intervals. The number of data points in each interval is shown in Figure 4. The fractal dimension found for the finely gridded data for the same k-interval as in the left Figure 3 is $D = 2.47 \pm 0.01$ ($R = 0.9996$). This is smaller than $D = 2.73 \pm 0.05$ obtained for the coarse gridding (Figure 3, left) as it should be expected by mathematical reasons discussed in the text.

dimension, which is the case shown in Figure 7.

4.3 Summary of Result Uncertainties

The notion of fractal dimension is applicable to definite scale intervals, which should be given along with the final results. Obviously, intersubject comparison is only meaningful if equal intervals are applied. There may be several ways to equalize them. The simplest would be to always select equal k-intervals. This is however less meaningful for cortices with a significant difference in size. A better way would be to appropriately rescale the considered k-interval. Note that an image scaling does not change its fractal dimension up to the obvious restriction of the finite sampling. This uncertainty produces an error of a few per cent, which is comparable with the fit accuracy.

Another uncertainty stems from the above discussed way of averaging, which yields the $F(k)$ curve (Figure 7). As it is shown by the considered example, the fractal dimension can change by up to 10% for the extreme case presented in Figure 7. The averaging way should obviously be the same to enable intersubject comparison.

The present study shows the method's feasibility and reports first results for two healthy subjects. A larger number of subjects, possible correlations with brain diseases, as well as the issue of optimal averaging will be reported elsewhere.

4.4 Comparison with other Methods

Let us discuss the relation of the present method to known approaches in characterizing the cortex folding. Hofman (Hofman, 1991), has observed that the convoluted brains of terrestrial mammals possess an overproportional increase in the total cortical surface as a function of the brain volume, which is an indication of the fractal geometry. This areametric approach was further used by Majumdar and Prasad (Majumdar and Prasad, 1988) and Free et al. (Free et al., 1996). Appropriate computational methods imply counting the smoothed cortical area as a function of the smoothing extent. The smoothing hides fine details, thus providing a probe for different spatial scales. Its specific realization used in (Free et al., 1996) was a dilation of the grey-white matter interface. This approach suffers from the abuttal of gyri (Free et al., 1996), which explains its application to only the inner cortical surface (Free et al., 1996). This requires intensive computations thus yielding a restricted amount of points for fitting the fractal dimension (for example, their result is based on five data points). The good fit quality obtained in (Free et al., 1996) does not show this restriction as a disadvantage. However it does not allow to probe the cortical geometry over all scales.

In contrast, the present method is based on a volumetric approach. It avoids the problem of defining the interface areas in discretized three-dimensional images. The high computational efficiency allows for visualizing the grey matter geometry over all scales as shown, for example, in Figure 3.

The price for these different advantages is an incomplete understanding of the relation between results of the areametric and the volumetric calculations of the fractal dimension. Basically, both methods should yield similar results. Consider, for example, an idealized situation of the cortex with a constant thickness. Smoothing implies that the convolved cortex is replaced with a flat slightly curved surface at fine spatial scale up to some size R (Figure 8). The surface structure at coarser scales is preserved. The original surface area $a(0)$ inside the smoothing sphere can be estimated as the volume inside this sphere divided by the cortex thickness Δ. This is $a(0) \propto R^D/\Delta$ according to the definition of the fractal dimension. This area is replaced upon smoothing by $a(R) \propto R^2/\Delta$, which corresponds to an unfolded surface. Thus the surface area inside the smoothing sphere is reduced by a factor $a(R)/a(0) \propto R^{2-D}$. As this estimate is applicable to each cortex element, the same relation holds for the whole smoothed surface area. This is exactly the formula used by Free et al. (Free et al., 1996) to measure the fractal dimension.

This example supports the idea that the areametric and the volumetric approaches give close results for the fractal dimension. It is though difficult to say how close the results should be. First, the cortex thickness is not constant. Second, any practical realization of the areametric approach needs to specify a way of smoothing. The implementation in (Free et al., 1996) involves

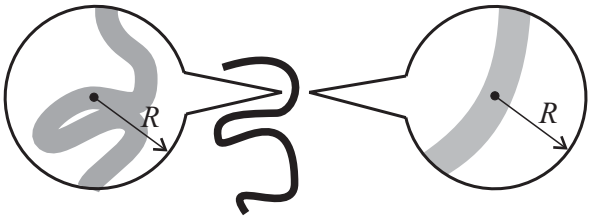

Fig. 8.
An illustration of the smoothing of a convolved surface. The extent of smoothing is set by a sphere of radius R, which is shown before (left) and after the smoothing (right). Inside this sphere the convolved surface is replaced with a piece of a flat one (transition from left to right in the Figure). At larger scales the overall surface shape is preserved (figure in the middle). The black dots represent a cortex element put in the origin of the sphere.

non-analytical operations such as thresholding, which hinders a precise analytical analysis. Third, the available areametric results are obtained for either inner or outer cortical surface, while the present method works with the whole cortical volume. By these reasons, it should be expected that the discussed methods yield fractal dimensions with numerically small, but systematic deviations from each other.

This is supported by the available results (Majumdar and Prasad, 1988; Free et al., 1996). The fractal dimension found in (Free et al., 1996) for the inner cortical surface is 2.30 ± 0.01, which is reasonably smaller that the volumetric one found in the present study. One can expect that the volumetric result is closer to the outer cortical area, as the latter is larger. The fractal dimension of this interface was found to be 2.60 ± 0.05 (Majumdar and Prasad, 1988). The agreement with the presented results $D = 2.74 \pm 0.05$ and $D = 2.69 \pm 0.05$ is better than it could be expected in view of the above discussed systematic difference in the computation methods.

An established measure of the cortex folding is the gyrification index (GI) (Zilles et al., 1988). It is based on length measurements in brain sections. The gyrification index for a section is the ratio of the total length of the dissected cortical area to the length of outer contour around the section. The mean GI for a hemisphere is defined as the ratio of sum over sections of all total lengths to the sum of all outer contour lengths.

The notions of both the fractal dimension and the GI relay on a comparison between the overall size of the brain and the size of the folded cortex. The similarity ends here though. Calculations of GI make use of the extreme of the largest scale (the outer contour) and of the finest scale, at which the total cortical section length is measured. Since the outer contour cannot be treated statistically, it is difficult to deduce a mathematical relation between the GI and the cortical fractal dimension. It would be in spirit of the fractal calculus

to consider the contours, which are smoothed to different extent. In practice, the GI focuses on rather location-specific information without referring to variable spatial scales.

5 Summary

An analysis of the cortical geometry is performed in all spatial scales. It shows that the brain grey matter does possess a self-similarity range down to details of about 2.5 mm. The fractal dimension in this range reasonably agrees with previously reported values. The calculational method is based on the Fourier transform of segmented three-dimensional high-resolved magnetic resonance images. The resulted computational algorithm is extremely effective and involves only standard methods of classical mathematics.

Acknowledgement

One of us (V.G.K.) acknowledges the kind help of D. Gembris, S. Wiese, M. Zaitsev and a useful discussion with K. Zilles. We thank K. Rodenacker for important contributions to the segmentation procedure. This work was supported in part by DFG SFB386.

Appendix: Equivalence of Direct and Fourier Determination of Fractal Dimension

The presented proof is a modification of one given in (Liu, 1986) for the context of brain MRI.

The function $F(k)$ defined in eq. (3) has the following explicit form:

$$\begin{aligned} F(k) &= \int f(\mathbf{k}) f^*(\mathbf{k}) \frac{d\Omega_k}{4\pi} \\ &= \int f(\mathbf{r}) f(\mathbf{r}') e^{-i\mathbf{k}(\mathbf{r}-\mathbf{r}')} d\mathbf{r} d\mathbf{r}' \frac{d\Omega_k}{4\pi}, \end{aligned} \tag{5}$$

where $f(\mathbf{r})$ is unity in cortex and zero otherwise, $d\Omega_k$ performs integration over the orientations of $\mathbf{k}$. Let us change the integration variable from $\mathbf{r}'$ to $\Delta\mathbf{r} = \mathbf{r} - \mathbf{r}'$ and integrate first over $\mathbf{r}$. This gives

$$\begin{aligned} F(k) &= \int f(\mathbf{r}) f(\mathbf{r} + \Delta\mathbf{r}) e^{-i\mathbf{k}\Delta\mathbf{r}} d\Delta\mathbf{r} d\mathbf{r} \frac{d\Omega_k}{4\pi} \\ &= \int \rho(\Delta\mathbf{r}) e^{-i\mathbf{k}\Delta\mathbf{r}} d\Delta\mathbf{r} \frac{d\Omega_k}{4\pi}, \end{aligned} \tag{6}$$

where $\rho(\Delta\mathbf{r})$ is the two-point correlation function of the cortex for the given spacing $\Delta\mathbf{r}$. Now we use the property of the Fourier transform that a rotation in the source results in the opposite rotation of the image. To do it accurately, let us define a fixed vector $\mathbf{k}_0$ and obtain all orientations of the integration variable $\mathbf{k}$ as $\mathbf{k} = O\mathbf{k}_0$, where O is a rotation matrix. We obtain

$$\begin{aligned} F(k) &= \int \rho(\Delta\mathbf{r}) e^{-i\mathbf{k}_0 O^{-1}\Delta\mathbf{r}} d\Delta\mathbf{r} \frac{d\Omega_k}{4\pi} \\ &= \int \rho(O\Delta\mathbf{r}') e^{-i\mathbf{k}_0\Delta\mathbf{r}'} d\Delta\mathbf{r}' \frac{d\Omega_k}{4\pi}, \end{aligned} \tag{7}$$

where we have changed the integration variable $\Delta\mathbf{r}$ to $\Delta\mathbf{r}' = O^{-1}\Delta\mathbf{r}$ and used the property $O^t = O^{-1}$. Note that Ω_k still defines the rotation angles of the matrix O. Thus the integration over Ω_k performs the averaging of $\rho(O\Delta\mathbf{r}')$ over the orientations of its argument. This gives the definition of the fractal dimension D:

$$\int \rho(\Delta\mathbf{r}) \frac{d\Omega_k}{4\pi} \propto (\Delta r)^{D-1}. \tag{8}$$

Substituting this into (eq. (7)) and calculating the Fourier integral we finally obtain that

$$F(k) \propto k^{-D} \tag{9}$$

if D does not depend on $\Delta\mathbf{r}$.

References

Ashburner, J., Friston, K., 2000. Voxel-based morphometry – the methods. NeuroImage 11, 805–821.

Chuang, K., Valentino, D., Huang, H., 1991. Measuring the fractal dimension using 3D technique. Proc. SPIE Image Process 1445, 341–347.

Cocosco, C., Kollokian, V., Kwan, K., et. al., 1997. Brainweb: Online interface to a 3D MRI simulated brain database. NeuroImage 5, 425.

Dale, A., Fischl, B., Sereno, M., 1999. Cortical surface-based analysis. NeuroImage 9, 179–194.

Free, S., Sisodiya, S., Cook, M., Fish, D., Shorvon, S., 1996. Three-dimensional fractal analysis of the white matter surface from magnetic resonance images of the human brain. Cerebral Cortex 6, 830.

Gunning-Dixon, F., Head, D., Mc Quain, J., Acker, J., Raz, N., 1998. Differential aging of the human striatum: a prospective MR imaging study. AJNR Am J Neuroradiol 19, 1501–1507.

Hahn, K., Rodenacker, K., Auer, D., 2000. Segmentierung des Gehirns auf der Basis von MR-Daten. In: BVM 2000. Springer, pp. 86–90.

Hahn, K., Rodenacker, K., Auer, D., 2001a. Cortex homogenization for intensity segmentation – an alternative. NeuroImage 13/6, 141.

Hahn, K., Rodenacker, K., Kempe, A. e. a., 2001b. Intensitätssegmentierung von T1-gewichteten MR Gehirndaten über die Homogenisierung der grauen oder der weißen Materie - eine vergleichende Studie. In: BVM 2001. Springer, pp. 207–211.

Hofman, M., 1991. The fractal geometry of convoluted brains. J. Hirnforschung 32, 103.

Kaufmann, C., Schuld, A., Pollmächer, T., Auer, D., 2002. Reduced cortical gray matter in narcolepsy: Preliminary findings with voxel-based morphometry. Neurology 58, 1852–1855.

Kwan, K., Evans, A., Pike, G., 1996. An extensible MRI simulator for post-processing evaluation. In: Proc. Conference on Visualistion in Biomedical Computing. pp. 135–140.

Liu, S., 1986. Fractals and their Applications in Condensed Matter Physics. Academic Press.

Majumdar, S., Prasad, R., 1988. The fractal dimension of cerebral surfaces using magnetic resonance imaging. Comput. Phys. Nov/Dec, 69–73.

Zilles, K., Amstrong, E., Schleicher, A., Kretschmann, H., 1988. The human pattern of gyrification in the cerebral cortex. Anat Embriol 179, 173–179.